GEOPHYSICAL RESEARCH LETTERS, VOL. 18, NO. 7, PAGES 1357-1360, JULY 1991

OBSERVATIONS OF O_2 ($^1\Sigma$) AND OH NIGHTGLOW DURING THE ALOHA-90 CAMPAIGN

Jeng-Hwa Yee, Rick Niciejewski and Ming Zhao Luo

Space Physics Research Laboratory, University of Michigan

Abstract. Two spectroscopic instruments, a 1/4 meter Ebert-Fastie spectrometer and a Michelson interferometer, were flown aboard the NCAR Electra during the ALOHA-90 campaign. These instruments were designed to carry out measurements of the brightnesses and rotational temperatures of the O_2 Atmospheric (0-1) band and several OH Meinel bands simultaneously with sodium lidar observations. The spectrometer results taken during the nights of March 25 and March 31 are reported. Wave-like oscillations in both O_2 and OH airglow brightnesses were clearly present during both flights and a strong positive correlation of OH band brightness with sodium column density was found. A slightly weaker correlation of O_2 band brightness with sodium column density was also detected. The measured brightness ratio between the OH (7-4) and (7-3) bands is found to be 11.2±0.3, which is in good agreement with the calculated ratios of 12.8 by Mies [1974] and 10.2 by Langhoff et al. [1986].

Introduction

The atmospheric gravity wave grows exponentially with altitude before breaking, saturating or dissipating energy. It is this friction force which provides the deceleration for the mean wind and affects the circulation of the atmosphere [Leovy, 1964]. The same effect also changes the eddy mixing in the region and modifies the vertical distribution of the minor constituents, such as the atomic oxygen density [Lindzen, 1981; Weinstock; 1982; Garcia and Solomon, 1985]. Since the $O_2(^1\Sigma_g)$ Atmospheric and OH ($^2\Pi$) Meinel bands emissions are products directly related to the atomic oxygen and originate at two different altitudes, these two optical emissions can be used as a remote sensing probe to study gravity waves [Krassovsky, 1972; Krassovsky and Shagaev, 1974; Hines and Tarasick, 1987].

Two instruments, a 1/4 meter Ebert-Fastie spectrometer and a Michelson interferometer, participated in the ALOHA-90 campaign aboard the NCAR-Electra with the sodium lidar. These instrument were designed to provide simultaneous measurements of the brightnesses and rotational temperatures of the O_2 Atmospheric and several OH Meinel bands emissions. In this letter we will present the brightness results obtained on March 25 (a North-South flight) and on March 31 (an East-West flight). Niciejewski and Yee [1991] will describe the temperature results obtained on March 31 flight. Our brightness observations indicate the presence of strong gravity wave activities and show a strong correlation with sodium column densities.

Paper number 91GL01295
0094-8534/91/91GL-01295$3.00

Instrument Description

The University of Michigan Visible and Near-infrared Spectrometer is a 1/4 meter Ebert-Fastie spectrometer using a Charge Coupled Device (CCD) detector. It uses a holographic grating with 1200 lines/mm operating in the first order. The spectrum is imaged onto an area-scan CCD detector and binned to obtain the spectrum of interest. The detector system is a modified Photometric camera head with a Thompson TH7882 CCD chip. The use of an array detector allows the entire 225Å spectral region to be sampled without any grating movement. The CCD was electronically binned to obtain 128 spectral channels (~1.74Å per channel) and the electronic signal was sampled every 30 seconds by an analog-to-digital converter that produced one digital count per 15.6 electrons.

The instrument has a field of view of 0.07 x 2.52 degrees defined by the telescope objective lens (f/5) with a focal length of 150 mm and an input slit of 0.19 x 6.62 mm. This corresponds to a spatial coverage of approximately 0.12 x 4.18 km for an emission originating near 95 km such as the O_2 Atmospheric band emission. The slit width also sets the spectral resolution to be ~10Å. The CCD chip was cooled to ~-50 C by using a three-stage thermal-electric cooler coupled with flowing liquid coolant (~-30 C). The quantum efficiency of the Thompson TH7882 CCD used in our spectrometer is ~20% near 8600Å, giving an absolute sensitivity per channel of ~3.1 electrons/sec/R/Å at 8600Å.

Observational Results and Discussion

Figure 1 shows an example of the measured nightglow spectrum averaged over 6 minutes on the night of March 25, 1990 obtained at 11:48 UT. The P and R branches of the O_2

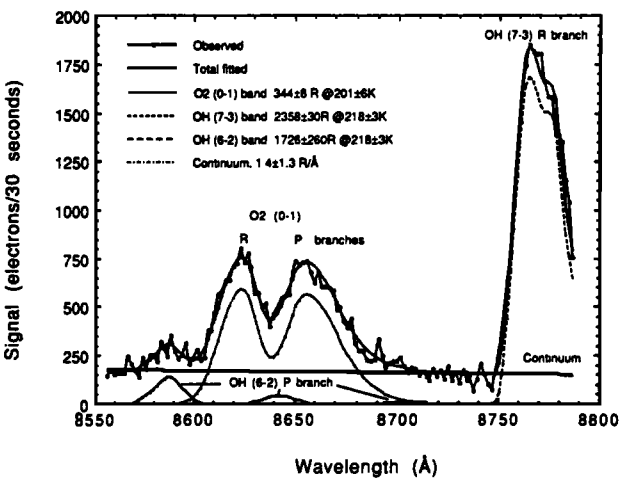

Fig. 1 A 6-minute averaged spectrum and individual contributions from various O_2 and OH emission bands obtained at 11:48 UT on the night of March 25, 1990.

Atmospheric band emission are clearly revealed. The spectral feature appearing near 8760Å is the R branch of the OH Meinel (7-3) emission. The spectral feature near 8590Å represents the $P_1(7)$ and $P_2(7)$ lines of the OH Meinel (6-2) emission. The CCD temperature was constantly regulated and monitored during the entire observation period. The thermal background was sampled every integration period (30 seconds) and was easily removed. A non-linear least square fitting technique was used to recover the brightnesses and rotational temperatures of the O_2 Atmospheric (0-1) band and the OH Meinel (7-3) and (6-2) band emissions. Also shown in Figure 1 are the contributions from each individual emitter, O_2 ($^1\Sigma_g$), OH($^2\Pi$), and the continuum with fitted brightnesses and corresponding temperatures. The line positions of the O_2 and OH emissions are obtained from Babcock and Herzberg [1948], Coxon [1980], and Coxon and Foster [1982], respectively. The individual line brightness of the O_2 Atmospheric band emission as a function of rotational temperature is determined by using the Honl-London factors of Schlapp [1937]. Those of the OH (7-3) and (6-2) band emissions are obtained from the calculation of Mies [1974].

Figure 2 shows the measured brightnesses of the O_2 Atmospheric (0-1) band and the OH (7-3) band emissions as a function of universal time throughout the flight on March 25, 1990. On this night the Electra left Maui at ~8:30 UT flying due south and turned northward near Christmas Island (~2 N) at ~12:15 UT. Wavelike oscillations were seen in both the O_2 and OH emissions and a correlation between the two was clear. In addition, both emissions show a distinct enhancement near 12:00 UT when the Electra was close to the equator. This phenomenon was also observed on another north-south flight on March 22. During the northbound flight on March 25, the OH brightness generally decreased with time. Near 14:30 UT, while the OH brightness still decreased, a sharp increase in the O_2 brightness was detected. This O_2 brightness enhancement was also reported by the airglow imager stationed at Haleakala [Hecht and Walterscheid, 1991]. In addition, a striking correlation of the OH brightness with the sodium column abundance between 80 and 90 km, the altitude region where the OH emission originated, was observed (Figure 3a). A less pronounced correlation between O_2 emission and sodium abundance between 90 and 100 km was also found (Figure 3b). The O_2 emission enhancement observed near 14:30 UT was followed by a sharp increase in the sodium abundance, with a delay of approximately 30 minutes. This increase was

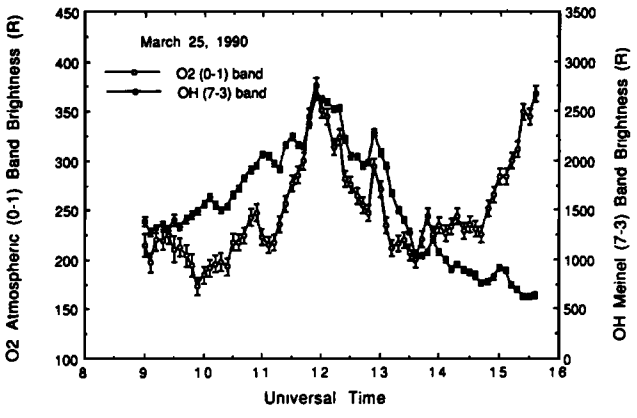

Fig. 2 Measured brightnesses of the O_2 Atmospheric (0-1) band and the OH (7-3) band emissions on March 25.

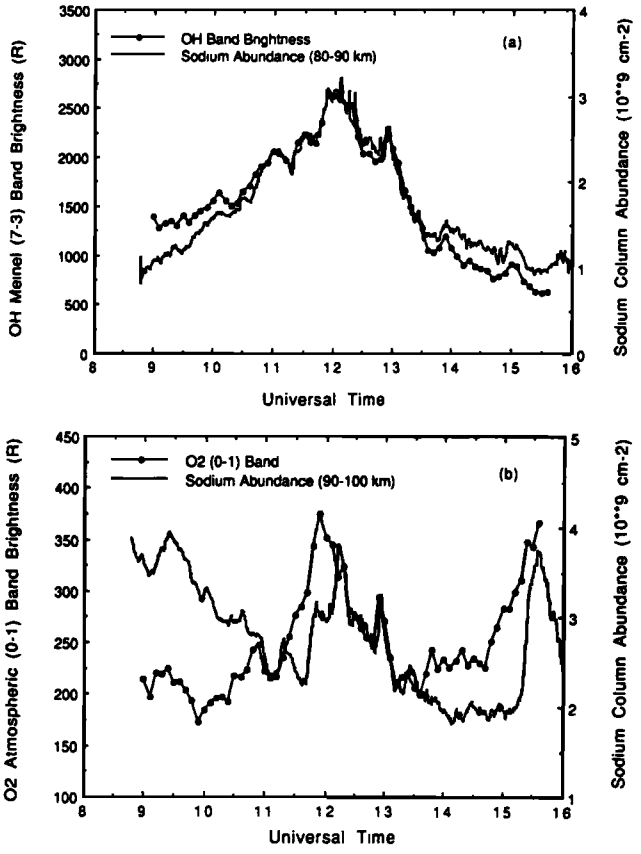

Fig. 3 Correlation of (a) OH and (b) O_2 nightglow emissions with the sodium column abundance on March 25.

associated with the formation of a sporadic sodium event described by Gardner et al. [1991].

The magnitude of the small-scale wavelike perturbations can be obtained by carefully removing the slow-varying trend. This trend is determined by first subtracting the linear component, subjecting the data to a low pass filter by employing a fast Fourier transform, and finally recombining the results with the linear component. The small-scale perturbations in OH (7-3) band brightness obtained in this way are presented in Figure 4a as a function of universal time (UT) throughout the flight, and the wave signatures are clearly revealed. A wave with a period of approximately 1 hour and an amplitude of ~100-200R (~10%) can be clearly seen during both legs of the flight. Wave periods can be determined from the power spectral densities shown in Figure 4b, obtained by using the Maximum Entropy Method (MEM). It indicates that the waves may not be monochromatic and waves with periods of ~1 hour (both the southbound and northbound legs) and ~0.4 hour (the southbound leg) are present. Due to the aircraft motion and the background winds in the emission altitudes, the observed periods are Doppler shifted from the real wave periods and differ slightly between the two legs [Kwon et al., 1990]. Because the aircraft velocity is known (~580 km/hour), one can solve for the intrinsic wavelength and the observed phase velocity along the flight path following the approach used by Kwon et al. [1990]. However, since there are two periods observed in the southbound flight, we do not know which one might be associated with the 0.94 hour wave observed in the northbound flight. As a result, we cannot

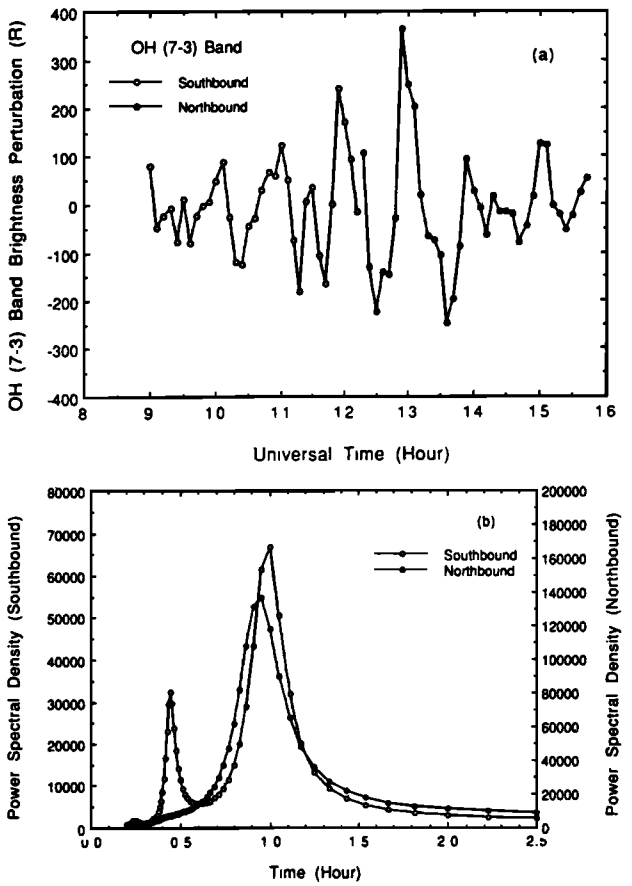

Fig. 4 (a) OH (7-3) band brightness perturbations as a function of time measured after slow-variation trends are removed, (b) The power density spectra of the brightness perturbations for both the southbound and northbound flights.

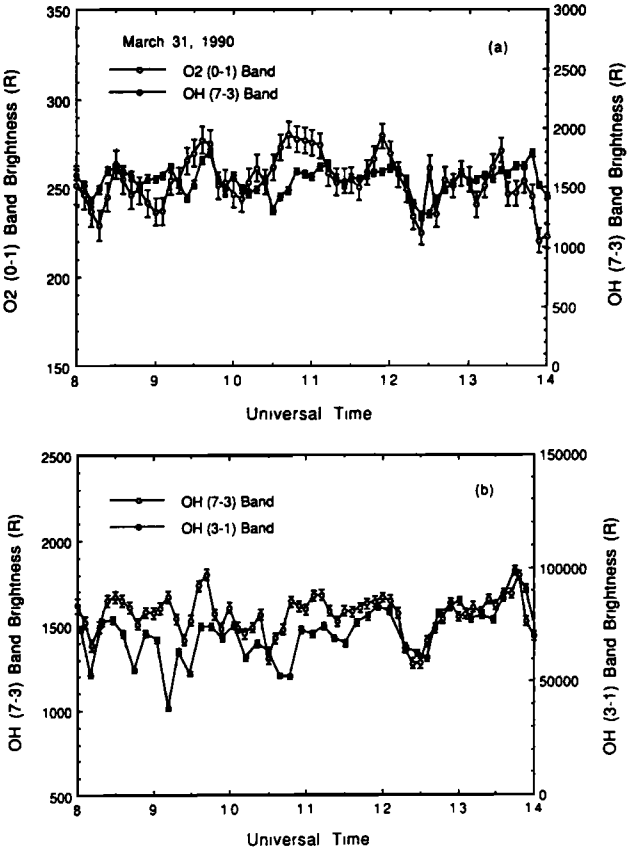

Fig. 5 (a) Measured brightnesses of the O_2 Atmospheric (0-1) band and the OH (7-3) band emissions on March 31. (b) Correlation between the OH (7-3) and (3-1) band brightnesses from the measurements of the grating spectrometer and Michelson Interferometer.

conclusively identify the wave. Using the combination of 0.94 hour (northbound) and 1.0 hour (southbound), we found that the intrinsic wavelength in the meridional direction is ~560 km and the phase velocity is ~6 m/sec southward. The other set of possible observed periods, 0.94 hour (northbound) and 0.4 hour (southbound), gives an intrinsic wave wavelength in the meridional direction of ~330 km and a phase velocity of ~70 m/s northward. The hour-averaged meridional wind velocity at 86 km (near the peak of the OH emission) measured at Christmas Island (2°N, 157° W) on March 25 varied between 0 and 20 m/s northward [Vincent and Lesicar, 1991]. By subtracting a mean background wind velocity of ~10 m/s northward, the two possible intrinsic meridional phase velocities are calculated to be ~16 m/s southward (wave period of ~10 hours) and ~60 m/s northward (wave period of ~1.5 hour) respectively. The 10-hour wave found here is usually difficult to observe from groundbased observations. It should be noted that the accuracies of the wave parameters derived in this approach depend strongly on the observed periods determined from Figure 4b and the validity of the assumption that the wave extended greater than 2000 km and lasted at least six hours.

Figure 5a presents the measured O_2 and OH brightnesses for March 31. On this night, the Electra flew westward from Maui near 8:30 UT toward the International Date Line and turned eastward near 11:40 UT. The airglow emissions exhibit apparent wavelike oscillations similar to those observed on the night of March 25. Although it is not shown here, a correlation of the airglow emissions with sodium abundances was also found. The increases in airglow brightnesses and sodium abundances which were observed near 12:00 UT on the north-south flights of March 22 and 25 were not present on this east-west flight. If these increases are associated with a latitudinal effect, they are inconsistent with the observed latitudinal distribution of the O(^{1}S) green line brightness during equinox [Cogger et al., 1981; Yee and Abreu, 1987] and the 2-D model prediction of Garcia and Solomon [1985].

A Michelson interferometer was also aboard the Electra and was designed to measure the brightnesses and rotational temperatures of several vibrational-rotational transitions within the ground state of OH. Descriptions of the instrument and data analysis technique used to recover the band brightness and temperature are given by Niciejewski and Yee [1991]. The Michelson and the grating spectrometer had the same pointing geometry and both were absolutely calibrated before the flights using the same low brightness source as described by Niciejewski and Yee [1991]. Figure 5b presents the measured brightnesses of the OH Meinel (3-1) and (7-3) bands obtained simultaneously by the two instruments. The two emissions correlate very well during the night and the brightness ratio I(7-3)/I(3-1) seems to increase slowly with time, suggesting slow temporal compositional changes in the

emission region and possible changes in the emission altitude.

In addition to the observations of the OH (7-3) and (3-1) bands, we have also obtained simultaneous measurements of the (6-2), (7-4), and (8-5) bands. Table 1 gives the 3-hour averaged brightnesses of these bands taken between 11:00 UT and 14:00 UT. Since the brightness of the (6-2) band emission is mainly obtained from the spectroscopic measurements of the P(N≥7) lines as shown in Figure 2, it should be interpreted

Table 1: Measured OH band Brightnesses

Band	Brightness (kR)	Source
(8-5)	23.0±1.0	Michelson
(7-4)	17.5±0.5	Michelson
(7-3)	1.570±0.005	Grating
(6-2)	1.18±0.04	Grating
(3-1)	79.0±0.7	Michelson

with care considering the possible incomplete rotational-translational (R-T) thermalization of OH reported by Pendleton et al. [1989]. For the unresolved R branch of the (7-3) band, it also contains several lines from the levels which may not be thermalized. However, this effect may be insignificant due to their relative weakness. Our measured brightness ratio between the (7-4) and (7-3) bands was found to be 11.2±0.3, which is in good agreement with the calculated ratios of 12.8 by Mies [1974] and 10.2 by Langhoff et al. [1986].

Acknowledgments The authors would like to thank Prof. C. S. Gardner, Tim Kane and Chris Hostetler for providing the sodium data. This research was primarily supported by National Science Foundation grants ATM-8822530 and ATM-8901367. The grating spectrometer was constructed under the support of Air Force Geophysics Laboratory.

References

Babcock. H.D., and L. Herzberg, Fine structure of the red system of Atmospheric oxygen bands, Astrophys. J., 108, 167, 1948.

Coxon, J. A. Optimum molecular constants and term values for the OH $X^2\Pi(v\leq5)$ and $A^2\Sigma^+(v\leq3)$ states of OH, Can. J. Phys., 58, 933, 1980.

Coxon, J. A. and S. C. Foster, Rotational analysis of hydroxyl vibration-rotation emission bands: Molecular constants for OH $X^2\Pi$, $6\leq v\leq10$, Can. J. Phys., 60, 41, 1982.

Garcia, R. R. and S. Solomon, The effect of breaking gravity waves on the dynamics and chemical compositions of the mesosphere and lower thermosphere., J. Geophys. Res., 90, 3850, 1985.

Gardner, C.S., T. J. Kane, J. H. Yee, R. J. Niciejewski, J. H. Hecht, R. L .Walterscheid, R. P. Lowe, and D.N. Turnbull, Formation characteristics of sporadic Na Layers observed simultaneously by lidar and airglow instruments during ALOHA-90, Geophys. Res. Lett.,this issue, 1991.

Hecht, J. H. and R. L. Walterscheid, Observations of the OH Meinel (6,2) and O_2 Atmospheric (0,1) nightglow emissions from Maui during the ALOHA-90 Campaign, Geophys. Res. Lett., this issue, 1991.

Hines, C.O.and D. W. Tarasick, On the detection and utilization of gravity waves in airglow studies, Planet. Space Sci., 35, 851, 1987.

Krassovsky,V.I., Infrasonic variations of OH emission in the upper atmosphere, Ann. Geophys. Res., 72, 2972, 1972.

Krassovsky,V.I.and M.V.Shagaev, Optical methods of recording acoustic or gravity waves in the upper atmosphere. J. Atmos. Terr. Phys. 36, 373, 1974.

Kwon, K. J., D. S. Senft, and C. S. Gardner, Airborne sodium lidar observations of horizontal and vertical wave number spectra of mesopause density and wind perturbations, J. Geophys. Res., 95, 13,737, 1990.

Langhoff, S.R., H.J. Werner and P. Rosmus, Theoretical Transition Probabilities for the OH Meinel System, J. Mol. Spectro., 118, 507, 1986.

Leovy, C. Simple models of thermally driven mesospheric circulation, J. Atm. Sci., 21, 327, 1964.

Lindzen, R. S., Turbulence and stress owing to gravity wave and tidal break-down, J. Geophys. Res., 86, 9707, 1981.

Mies, F.H. Calculated Vibrational Transition Probabilities of $OH(X^2\Pi)$, J. Mole. Spectro., 53, 150, 1974.

Niciejewski and J. H. Yee, Airglow rotational temperature measurements during the ALOHA campaign, Geophys. Res. Lett., this issue, 1991.

Pendleton, Jr., W., P. Espy, D. Baker, A. Steed, and M. Fetrow, Observation of OH Meinel (7,4) P(N"=13) transitions in the night airglow, J. Geophys. Res., 94, 505, 1989.

Schlapp, R. Fine structure in the $X^3\Sigma_g^-$ ground states of the oxygen molecule, and the rotational intensity distribution in the atmospheric oxygen band, Phys. Rev., 51, 342, 1937.

Vincent, R. A. and K. Lesicar, Mean winds, tides and gravity waves in the upper middle atmosphere during ALOHA-90, Geophys. Res. Lett., this issue, 1991.

Weinstock, J., Nonlinear theory of gravity waves: momentum deposition, generalized Rayleigh friction, and diffusion, J. Atmos. Sci., 39, 1698, 1982.

Yee, J. H. and Abreu, V. J. Mesospheric 5577Å green line and atmospheric motions - Atmosphere Explorer satellite Observations, Planet. Space Sci., 35, 1389, 1987.

J. H. Yee, Rick Niciejewski and Ming Zhao Luo, Space Physics Research Laboratory, 2455 Hayward Street, University of Michigan, Ann Arbor, MI 48109.

Received: April 8,1991
Accepted: May 7, 1991.